Techno-economic assessment of hybrid CSP-biogas power plants

Mario Petrollese* and Daniele Cocco

Department of Mechanical, Chemical and Materials Engineering, University of Cagliari, Via Marengo, 2 09123 Cagliari, Italy.

* Corresponding Author: Mario Petrollese

petrollese@unica.it, Tel. ++39 070 6755118

Abstract:

This study aims to investigate the performance and economic benefits arising from the integration of concentrating solar power (CSP) plants with anaerobic digestion processes. To demonstrate the capabilities of hybrid CSP-biogas plants, the CSP section of the Ottana solar facility (Italy) is considered as a case study. A simulation model for the performance analysis of the hybrid system is developed, and the effects of variation in the volume of the anaerobic digester and the biogas storage capacity on the main performance indexes are evaluated. Furthermore, two different operating strategies for energy storage management are compared and the possible requirements for energy curtailment are analysed. Finally, a preliminary economic analysis is carried out. The results demonstrate the benefits and improvements in plant capacity factor and efficiency arising from proper sizing of the biogas section. Conversely, oversizing of the biogas section results in significant curtailments in biogas and/or solar field energy production, due to the limited storage capacity. Consequently, the optimal configuration, even from an economic point of view, is achieved by a biogas section of a size that is able to supply part (in the range of 10%–65%) of the nominal thermal power input required by the power block.

Keywords:

concentrating solar power, hybrid solar-biomass plant, anaerobic digestion, organic Rankine cycle, biogas production.

NOMENCLATURE

Symbols

A	area [m^2]
AC	annual costs [€/year]
c	specific heat [kJ/kgK]
E	energy [kWh]
h	specific enthalpy [kJ/kg]
IC	initial costs [€]
$\dot{m}$	mass flow rate [kg/s]
$\dot{Q}$	thermal power [kW]
T	temperature [°C]
U	overall heat transfer coefficient [J/(m^2 K)]
V	volume [m^3]
$\dot{W}$	electrical power [kW]
η	efficiency [-]
ρ	density [kg/m^3]
Δt	operating time [h]

Superscripts

d	design conditions
in	inlet side
out	outlet side

Subscripts

AMB	ambient conditions
AD	anaerobic digester
BB	biogas boiler
BG	biogas
BS	biogas storage
CT	cold tank
FL	flaring
HT	hot tank
SF	solar field

Acronyms

CSP	concentrating solar power
CHP	combined heat and power
FVW	fruit and vegetable wastes
HTF	heat transfer fluid
LCOE	levelised cost of energy
ORC	organic Rankine cycle
PTC	parabolic trough collector
TES	thermal energy storage

1. Introduction:

Concentrating solar power (CSP) is an effective technology for the conversion of solar energy into electricity. Unlike other renewable energy based technologies, CSP plants can provide flexibility for grid services, thereby facilitating the integration of variable-output renewable sources such as photovoltaic systems or wind turbines and contributing to the reliability of the transmission grid. However, the intermittent nature of solar energy limits the capacity factors achievable by these systems, and daily shut-downs are often unavoidable [1]. Although the inclusion of a thermal energy storage (TES) system can partially mitigate this drawback, the full dispatchability of these power generation plants would require very large solar fields and TES capacities, meaning that this is often unattainable [2].

A possible solution to overcome these limitations is the hybridisation of a CSP plant with other dispatchable sources. CSP technology can be readily integrated with other energy sources, leading to many potential benefits. Hybridisation allows to increase the dispatchability and reliability of CSP, improve its efficiency and reduce capital costs through the synergic contribution of the different energy sources [3]. Hybridised CSP plants have different types and levels of synergy, depending on the hybrid energy source, the location of the plant, the CSP technology and the plant configuration. A first hybrid solution is represented by the integration of a solar field with a conventional power plant fed by fossil fuels (coal or natural gas). A solar hybrid plant can utilise the existing infrastructure of a conventional power plant, thereby reducing the investment costs for the solar section [4]. In addition, although the solar contribution allows to reduce fuel consumption and therefore CO_2 emissions [5], the contribution from fossil fuels is usually predominant, and the reduction in fuel consumption and CO_2 emissions is therefore generally limited. Another interesting option for improving the dispatchability features without using a TES characterised by large storage capacity is related to the integration of the solar field with a suitable biomass boiler. Since both solar field and biomass boilers produce thermal energy with similar power outputs and temperature levels, these technologies are well suited for integration [3]. Moreover, since both of these energy sources are renewable and clean, this will result in a power supply with nearly zero carbon emissions. The possibility of sharing some of the system components (such as the power generation section), with significant savings in capital costs, may improve the attractiveness of small and medium power plants at distributed scale, which are usually characterised by lower conversion efficiencies and higher specific costs compared to large plants [6].

Several authors have analysed the potential of CSP-biomass hybridisation schemes from economic, technological and environmental perspectives. Peterseims et al. [7] investigated the generation potential and most suitable regions in Australia for 5–60 MW CSP hybrid plants using forestry residues, bagasse, stubble, wood waste and refuse-derived fuels, in locations characterised by high solar availability. The results highlighted the strong potential and the economic benefits arising from the realisation of such hybrid plants. San Miguel and Corona [8] used a standard life cycle assessment (LCA) methodology to investigate the environmental performance of a commercial 50 MW CSP plant in Spain that was hybridised with different auxiliary fuels (natural gas, biogas from an adjacent plant and biomethane withdrawn from the gas network). Their study demonstrated that the use of biogas rather than natural gas results in a significant improvement in the environmental performance of the installation, primarily due to the reduced impacts on natural land transformation, depletion of fossil resources, and climate change. Bai et al. [9] demonstrated the suitability of direct biomass combustion process for CSP hybridisation, highlighting how such hybrid processes contribute to ameliorating the thermodynamic system performance and the reduction of exergy losses within the steam generation process. Suresh et al. [10] developed a thermodynamic model for sizing a solar–biomass hybrid power plant based on a steam Rankine cycle. Their analysis revealed the importance of the proper sizing of the two sections to improve the power block efficiency, decrease the specific solar field area requirement and reduce the amount of biomass required. A techno-economic assessment of a hybrid solar-biomass power-generation system configuration composed of an externally fired gas-turbine fuelled by biomass and a bottoming organic Rankine cycle (ORC) plant was proposed by Pantaleo et al. [11]. Higher global conversion efficiencies were obtained by the hybrid configuration compared to the sole biomass unit but also higher investment costs, due to the current costs of CSP section, which makes the hybridization configuration a cost-effective investment only in the presence of a dedicated subsidy framework.

Based on the demonstrated potentiality of the hybrid concept, several hybrid CSP-biomass plant configurations have been proposed in the literature that differ depending on the desired plant size, the CSP and biomass technologies adopted and the goal, such as designing a novel hybrid system or investigating a retrofitting solution for an existing solar or biomass plant. The latter case is particularly relevant in the literature, and a number of recent studies have examined different hybrid schemes. Sterrer et al. [12] proposed the hybridisation of a CSP system with existing biomass plants based on an ORC power block operating in Salzburg, Austria. Parabolic through collectors (PTCs) were proposed for the indirect hybridisation of the system with the aim of maintaining thermal stability. Pantaleo et al. [13] also presented an hybrid CSP-biomass scheme for combined heat and power (CHP) generation, based on the incorporation of CSP into an existing biomass-only plant. Their hybrid plant consisted of a topping externally-fired gas turbine system, utilising thermal power from both PTCs and a biomass furnace in series. The exhaust heat from the gas turbine was then recovered as heat source for a bottoming ORC-CHP plant. The authors demonstrated the feasibility of the proposed system in terms of both its technical and economic performance. An analysis and comparison of different options for hybridising existing CSP plants with biomass through gasification for power generation was carried out by Milani et al. [14]. The results showed that all of the proposed configurations were feasible from a technical point of view, but for the same gasifier, different costs and technical performances were shown depending on the conceptual design chosen. In view of this, Oyekale et al. [15] proposed the retrofitting of existing CSP-ORC plants with a biomass combustion process. A parallel hybridisation scheme was proposed and analysed in which both a solar field with TES and a biomass furnace were able to independently satisfy the fractional thermal requirements of the power plant. The results demonstrated that in comparison with the current performance of the CSP-ORC plant, an important increase could be obtained by the proposed biomass retrofit in terms of the electrical efficiency and the annualised plant operating duration, as well as a reduction in the levelized cost of energy (LCOE).

From the foregoing, it could be inferred that the retrofitting of existing CSP plants with biomass systems (and vice versa) is a techno-economically favourable option. It is well known that various types of biomass are available (forest and agriculture residues, sugar crops, oilseed crops, etc.), as are different technologies for the energy conversion of biomass, such as direct combustion, gasification, pyrolysis, fermentation, oil extraction and anaerobic digestion. In particular, the latter is an efficient and sustainable option for treating organic waste materials, and produces a gas mixture (biogas) that is mainly composed of methane and carbon dioxide, which can be used to fuel boilers, diesel engines or gas turbines. In recent years, the hybridisation of CSP with biogas energy has attracted increasing amounts of attention, and its benefits have been highlighted by various studies [16]. In this regard, Kaushika et al. [17] proposed an integration between PTC and biogas plants and demonstrated the benefits of this hybridisation in terms of increasing the overall conversion efficiency and stability of the system. The improvements arising from this hybridisation in terms of power stability and power dispatchability were demonstrated by Zhang et al. [18]. Colmenar-Santos et al. [19] demonstrated the potential benefits in terms of improvements in operation time and better electrical production control arising from the hybridisation of CSP plants with biogas in comparison with salt storage systems. Furthermore, Soares and

Oliveira [20] analysed a biomass hybridisation scheme for a mini ORC power plant that was rated at 60 kW, with a heat source consisting of PTCs and a micro biogas boiler. The study was conducted as part of the REELCOOP project, which was co-funded by the European Union. The authors demonstrated that biomass hybridisation improved the technical performance of the system, increasing the annual energy yield by 6.2%.

As discussed above, the hybridisation of CSP plants with anaerobic digestion biogas plants has shown great potential, but further effort is required towards the definition of methodologies and best practices to follow in the design stage of these hybrid plants, and in particular if an existing CSP plant is to be retrofitted.

In this context, a novel configuration for the hybridisation of an existing medium-scale CSP power plant with a biogas system is proposed and analysed in this paper. Starting from the plant configuration of the CSP section of the Ottana solar facility (Italy), the effects of variation in the volume of the anaerobic digester and the biogas storage capacity on the average conversion efficiency and the overall capacity factor of the hybrid power plant are evaluated. Finally, a preliminary economic analysis is carried out to assess the economic benefits arising from hybridisation and the optimal configuration for minimising the energy production cost.

2. Methodology

2.1. Plant configuration

In order to examine the potential techno-economic benefits arising from the hybridisation of a medium-scale CSP plant (nominal power from hundreds of kW to few MW) with a biogas production system, an existing solar power plant in Ottana (Italy) is considered as a case study [21]. This solar facility has three main sections: a solar field, where the solar energy is concentrated to heat up the heat transfer fluid (HTF); a two-tank direct TES section, where the HTF is stored; and an ORC unit, where the thermal energy is converted into electricity. The solar field is composed of six lines of linear Fresnel collectors connected in parallel and aligned along the north-south direction, with an overall net collecting area of 8400 m^2. A commercial Therminol SP-I thermal oil is used as the HTF, and is also used as a storage medium in a two-tank TES system designed with an overall storage capacity of 15.2 MWh. The ORC unit is a Turboden 6HR Special, which is a 629 kW turbo generator based on a regenerative Rankine cycle and operated by an organic fluid (hexamethyldisiloxane, $C_6H_{18}OSi_2$). Table 1 gives the main design characteristics of the existing CSP plant.

Table 1 – Design characteristics of the solar field, TES system and ORC unit at the Ottana solar facility.

Solar field		**ORC unit**	
Net collecting area (A_{SF})	8400 m^2	Design HTF mass flow rate	11.05 kg/s
Focal length of the collector	4.97 m	Design inlet/outlet temperature	275/165°C
Length of the collector	99.45 m	Thermal power input ($\dot{Q}^{d}_{ORC}$)	3100 kW_t
Design optical efficiency (η^{d}_{OPT})	65.5%	Organic fluid	$C_6H_{18}OSi_2$
Cleanliness efficiency (η_{CLN})	98%	Cooling inlet temperature	25°C
TES system		Cooling outlet temperature	35°C
Storage capacity	15.4 MWh	Gross electrical power	664 kW
Design hot tank temperature (T^{d}_{HT})	275°C	Gross electrical efficiency	21.4%
Useful volume of the tank	330 m^3	Net electrical power	629 kW
Aspect ratio	0.32	Net electrical efficiency	20.3%

Starting with this solar plant configuration, the introduction of an additional renewable heat source, placed in parallel to the solar field and based on an anaerobic digestion process is proposed and analysed. In this way, a specified fraction of the thermal input required by the ORC unit is supplied by a dispatchable source (that is, the biogas plant), while the remaining fraction is satisfied by the solar field, depending on solar availability.
Figure 1 shows the conceptual scheme of the solar-biogas hybrid system. Fruit and vegetable wastes (FVW) are used as a single substrate in an anaerobic digester for the continuous production of biogas. The latter is then sent to a storage tank, if present, or directly burned in a biogas boiler, where a given HTF mass flow rate ($\dot{m}_{HTF,BB}$) is heated up to the nominal solar field exit temperature. The HTF circulating in the biogas boiler is then mixed with the HTF mass flow rate circulating in the solar field ($\dot{m}_{HTF,SF}$) by means of a three-way valve located upstream of the hot tank (HT). Finally, the ORC unit is directly supplied by the HTF stored in the hot tank. In this way, the HTF mass flow rate feeding the ORC unit ($\dot{m}_{HTF,ORC}$) is partially independent of the HTF mass flow rates introduced into the HT by the solar field and/or the biogas system, and can be managed based on the operational strategy adopted and the state of charge of the hot tank.

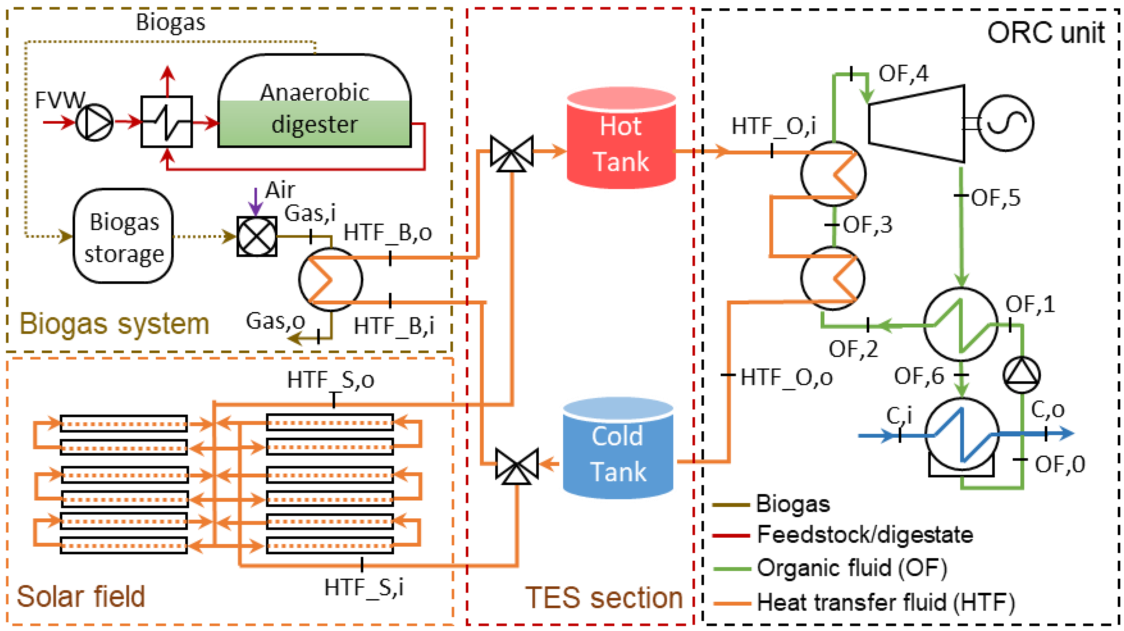

Figure 1 - Schematic of the hybrid CSP-biogas plant.

2.2. Mathematical model

The mathematical models used to simulate the main sections of the hybrid CSP-biogas plant are discussed in this section. Specific models to evaluate the performance of the solar field, biogas system, TES section and ORC unit under both design and off-design operating conditions are developed in a MATLAB environment. Since a biogas retrofit of an existing CSP plant is analysed in this study, only the sizing of the biogas section is required.

2.2.1. Solar field

The solar field performance is evaluated on an annual basis by means of a specifically developed simulation model, starting with hourly data on the direct normal irradiation (DNI), solar position, air temperature and wind speed. Firstly, the actual thermal power incident at the receiver $\dot{Q}_{INC}$ is calculated according to the following equation:

$$\dot{Q}_{INC} = DNI \cdot A_{SF} \cdot \eta_{OPT}^{d} \cdot IAM \cdot \eta_{END} \cdot \eta_{CLN} \tag{1}$$

where A_{SF} is the overall net collecting area, η_{OPT}^{d} is the design optical efficiency, IAM the incidence angle modifier, η_{END} the end-loss optical efficiency and η_{CLN} the surface cleanliness efficiency. Figure 2 shows the two IAM components in function of the longitudinal and transversal components θ_L and θ_T of the solar incidence angle θ [22]. End loss optical efficiency is evaluated as a function of the collector length, focal height and longitudinal component θ_L. The thermal power $\dot{Q}_{SF}$ transferred to the HTF is calculated by applying the receiver energy balance:

$$\dot{Q}_{SF} = \dot{Q}_{INC} - \dot{Q}_{REC,L} = \dot{m}_{HTF,SF} c_{HTF} \left(T_{HT}^{d} - T_{CT}\right) \tag{2}$$

where $\dot{Q}_{REC,L}$ represents the overall receiver thermal losses evaluated according to the specific correlations reported in [23]. Finally, a solar field control is introduced and the mass flow rate $\dot{m}_{HTF,SF}$ is adjusted to achieve the design temperature of the hot tank (T_{HT}^{d}), starting from the given HTF temperature inside the cold tank (T_{CT}).

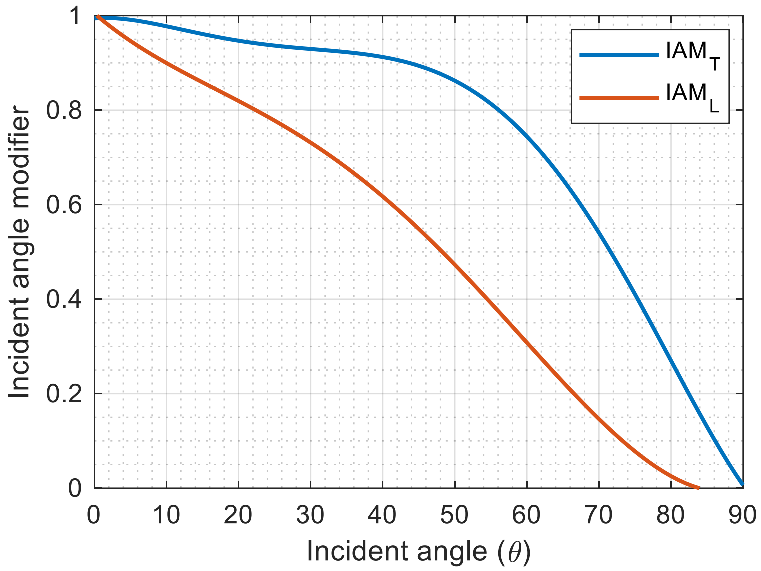

Figure 2 – Transversal and longitudinal incident angle modifiers (IAM$_T$ and IAM$_L$, respectively) [15].

2.2.2. Biogas system

As mentioned, the biogas is produced by an anaerobic digestion (AD) process using fruit and vegetable wastes. The choice of this substrate is related to the potential availability of these residues near to the plant location, although the proposed methodology can also be applied with other substrates. Unlike the other three sections, a suitable design for the biogas system is required in order to evaluate the yearly performance of the hybrid plant. Two main design parameters are introduced for the sizing of the biogas section:

- The design thermal power of the biogas boiler ($\dot{Q}_{BB}^{d}$), hereinafter expressed in relative terms compared to the ORC thermal power input under nominal conditions ($\dot{Q}_{ORC}^{d}$);
- The daily operation time of the biogas boiler (Δt_{BB}), expressed in hours.

Based on the assumption that the biogas boiler always works under nominal conditions, the daily volumetric flow rate (V_{BG}) of biogas is calculated by the following equation:

$$V_{BG} = \frac{\dot{Q}_{BB}^{d} \cdot \Delta t_{BB} \cdot 3600}{\rho_{BG} LHV_{BG} \eta_{BB}} \tag{3}$$

where ρ_{BG} and LHV_{BG} are the density and lower heating value of the biogas, respectively, and η_{BB} is the nominal biogas boiler efficiency. A suitable design of the anaerobic digester is therefore required to meet the biogas demand. In this study, the reactor is designed in accordance with the experimental results obtained from a pilot-scale AD system fed by FVW [24]. The main parameter used for the performance assessment of the AD process is the volumetric methane production rate (γ_V), defined as the ratio between the daily volumetric CH_4 production and the digester volume. According to [18], the CH_4 production rate can be expressed by the following equation:

$$\gamma_V = \frac{B_o S_o}{HRT}\left(1 - \frac{K}{(0.013T_{AD} - 0.129)HRT - 1 + K}\right) \tag{4}$$

where B_o is the ultimate methane yield, S_o is the influent total volatile solids (VS) concentration, HRT is the hydraulic retention time, K is a kinetic parameter and T_{AD} is the reactor temperature (here, set to 35°C, corresponding to mesophilic conditions for the digester). Consequently, the required digester volume is determined as:

$$V_{AD} = \frac{V_{BG} \cdot x_{CH4}}{\gamma_V} \tag{5}$$

where x_{CH4} is the mole fraction of CH_4 in the biogas. Obviously, the AD produces biogas continuously, meaning that for Δt_{BB} values lower than 24 hours, storage for the biogas is required in order to avoid flaring. A low-pressure floating biogas holder is used, for which the biogas storage volume (V_{BS}) is evaluated as a function of the daily operation time of the biogas boiler:

$$V_{BS} = V_{BG}\frac{(24 - \Delta t_{BB})}{24} \tag{6}$$

After the design stage is complete, the annual performance of the biogas system is evaluated using the mass and energy balance equations. It is assumed that the mass content inside the digester remains constant, meaning that for the entire operating period, the mass flow rate of feeding substrate ($\dot{m}_{FVW}$) is equal to the sum of the mass flow rates of the biogas produced in the anaerobic digester ($\dot{m}_{BG,AD}$) and the discharged digestates ($\dot{m}_{DIG}$):

$$\dot{m}_{FVW} = \dot{m}_{BG,AD} + \dot{m}_{DIG} \tag{7}$$

The energy balance is used to calculate the thermal energy required to keep the reactor temperature constant. According to [24], by neglecting minor contributions to the overall energy balance (such as the heat absorbed by the produced biogas), the heat ($\dot{Q}_{AD}$) required to keep the reactor temperature constant has two different components: the energy required to heat the feeding substrate from the ambient temperature to the digester temperature, and the energy required to balance the thermal losses:

$$\dot{Q}_{AD} = \dot{m}_{FVW} c_{FVW} (T_{AD} - T_{FVW}) + U_{AD} A_{AD} (T_{AD} - T_{AMB}) \tag{8}$$

where T_{FVW} is the temperature of the available substrate, U_{AD} is the overall heat transfer coefficient between the digester and the ambient temperature (T_{AMB}), and A_{AD} is the surface area of the reactor.

In the case where an external biogas storage is introduced, mass balance of this component is required in order to take into account the difference in the biogas mass flow rate produced by the anaerobic digester ($\dot{m}_{BG,AD}$) and that burned by the biogas boiler ($\dot{m}_{BG,BB}$):

$$\frac{\partial m_{BS}}{\partial t} = \dot{m}_{BG,AD} - \dot{m}_{BG,BB} - \dot{m}_{BG,FL} \tag{9}$$

where m_{BS} is the mass of biogas stored in the dedicated holder and $\dot{m}_{BG,FL}$ is the biogas mass flow rate that is flared, in the case where the volumetric content of the biogas inside the tank exceeds the design storage volume. Furthermore, it is assumed that the storage system is managed to ensure a completed charging/discharging cycle. Biogas storage is introduced because the mass flow rate continuously produced by the AD is lower than that required by the biogas boiler, and complete charging of the biogas storage is therefore imposed before the biogas boiler is started up. The biogas boiler is subsequently kept in operation until the biogas storage is completely discharged. Finally, the HTF mass flow rate circulating in the biogas boiler ($\dot{m}_{HTF,BB}$) is calculated starting from the energy balance of the biogas boiler, by assuming a boiler efficiency of 90% and an outlet temperature for the HTF equal to the design hot tank temperature (275°C):

$$\dot{m}_{BG,BB} LHV_{BG} \eta_{BB} = \dot{m}_{HTF,BB} c_{HTF} \left(T_{HT}^{d} - T_{CT}\right) \tag{10}$$

All the main design parameters used in both the design and the operating phases of the biogas section are listed in Table 2.

Table 2 - Main design data for the anaerobic digestion power plant.

Biogas		**Anaerobic digestion**	
Methane content (x_{CH4})	55%vol	Process temperature (T_{AD})	35°C
Lower heating value (LHV_{BG})	15.4 MJ/kg	Specific CH_4 production (B_o)	0.43 Nm^3/kg_{VS}
Biogas density (ρ_{BG})	1.28 kg/Nm^3	Hydraulic retention time (HRT)	30 days
Boiler efficiency (η_{BB})	0.90	Kinetic parameter (K)	0.9
Fruit and vegetable waste (FVW)		Reactor aspect ratio	0.4
FVW composition	TS = 8.7%wb	Insulation layer (rock wool)	0.1 m
	VS = 86%TS	Air convective heat transfer coefficient	10 W/m^2K
Volatile solid content (S_o)	75 kg_{VS}/m^3		

2.2.3. TES system

A two-tank direct TES system is considered: one is called the hot tank, and stores the hot fluid, while the other, called the cold tank, holds the exhausted cold fluid coming from the ORC unit. The TES system is modelled by considering the mass and energy balance for each tank (it is assumed that there is no thermal stratification inside each tank), as expressed in the following equations:

$$\frac{\partial m_{HT}}{\partial t} = \dot{m}_{HTF,BB} + \dot{m}_{HTF,SF} - \dot{m}_{HTF,ORC} \tag{11}$$

$$\frac{\partial m_{HT} h_{HT}}{\partial t} = \dot{m}_{HTF,BB} h_{HTF,BB}^{out} + \dot{m}_{HTF,SF} h_{HTF,SF}^{out} - \dot{m}_{HTF,ORC} h_{HT} - U_{TES} A_{TES} (T_{HT} - T_{AMB}) \tag{12}$$

$$\frac{\partial m_{CT}}{\partial t} = \dot{m}_{HTF,ORC} - \dot{m}_{HTF,BB} - \dot{m}_{HTF,SF} \tag{13}$$

$$\frac{\partial m_{CT} h_{CT}}{\partial t} = \dot{m}_{HTF,ORC} h_{HTF,ORC}^{out} - (\dot{m}_{HTF,BB} + \dot{m}_{HTF,SF}) h_{CT} - U_{TES} A_{TES} (T_{CT} - T_{AMB}) \tag{14}$$

where m_{HT} and m_{CT} are the masses of HTF stored in the hot and cold tanks, respectively, h_{HT} and h_{CT} are the average HTF enthalpies inside the hot and cold tanks, respectively, U_{TES} is the overall heat transfer coefficient between the stored fluid and the ambient air (determined by considering the convective air heat transfer and the thermal resistance of the wall) and A_{TES} is the external area of the tank. The TES heat losses due to imperfect insulation of the tanks are calculated by the last two of these parameters multiplied by the temperature difference between the stored HTF (T_{HT} or T_{CT}) and ambient air (T_{AMB}).

Since the hot tank is the heat source for the ORC unit, its mass and energy contents play a fundamental role in the definition of the operating strategy adopted for the turbo generator. In this study, it is assumed that the daily start-up of the ORC unit occurs when the HTF mass stored in the hot tank is able to continuously supply the ORC unit at nominal conditions for at least two hours.

Moreover, when the hot tank is completely charged (for example during summer days), suitable control over the HTF mass flow rate is required. Two different operating strategies are evaluated and compared:

a) Biogas priority: the thermal power rate of the biogas boiler is kept constant while the thermal power produced by the solar field is reduced through mirror defocusing in order to satisfy the energy balance of the TES section. The lack of solar field production gives the defocusing energy losses.

b) Solar priority: the biogas boiler operates at part-load conditions in order to rearrange the HTF mass flow rate circulating in the biogas system (no variations in the boiler efficiency has been assumed). Mirror defocusing is used only when the biogas boiler is completely switched off and the HTF mass flow rate produced by the solar field exceeds the maximum allowed value.

2.2.4. ORC unit

The ORC performance is evaluated through a calculation of the net conversion efficiency and the consequent net power production of the turbo generator. The ORC unit is designed to produce a net electrical power of 629 kW with a net efficiency of 20.3%. On the other hand, the ORC unit is often forced to operate at part-load conditions with a consequent decrease in efficiency. The main reason for fluctuation in the ORC performance is due to a reduction in the inlet HTF mass flow rate. Due to the large variability of the solar radiation, the HTF mass flow rate circulating in the solar field varies widely during the day, and the inclusion of a TES system can only partially mitigate these fluctuations. The ORC is therefore often fed with a reduced mass flow rate due to the limited mass of HTF stored, and the effect on the ORC efficiency is shown in Figure 3(a). A minimum HTF mass flow rate of 40% of the nominal value is imposed to avoid efficiency values that are too low, with the consequent shut-down of the turbo generator. Together with variations in the HTF mass flow rate, fluctuations in the HTF inlet temperature also occur, mainly due to unavoidable heat losses and the stratification of temperatures in the two storage tanks, with a significant effect on the ORC conversion efficiency, as shown in Figure 3(b). Obviously, the variations in the HTF mass flow rate and inlet temperature have an important effect on the HTF outlet temperature, and thus on the HTF temperature inside the cold tank, which feeds the solar field. Finally, the ORC performance also depends on the ambient temperature. Since the condensing heat is removed by dry coolers, the water temperature at the condenser inlet is directly related to the ambient temperature. Starting from the ambient temperature, the cooling water inlet temperature is calculated by assuming an approach temperature of 10°C. The effect of variation in the ambient temperature on the ORC efficiency is also shown in Figure 3(b). Overall, the net power produced by the ORC unit ($\dot{W}_{ORC}$) is calculated as:

$$\dot{W}_{ORC} = \eta_{ORC}\dot{m}_{HTF,ORC}c_{HTF}\left(T_{HT} - T_{HTF,ORC}^{out}\right) \tag{15}$$

where η_{ORC} is the actual ORC net efficiency, $\dot{m}_{HTF\_O}$ is the HTF mass flow rate feeding the ORC unit, T_{HT} is the temperature of the thermal oil stored in the hot tank and $T_{HTF\_O,o}$ is the HTF outlet temperature. The last of these parameters also depends on the HTF mass flow rate and the hot tank temperature. In fact, an increase in the temperature difference between the inlet and outlet sides of the ORC unit occurs with a reduction in the HTF mass flow rate, as shown in Figure 4. Consequently, the operation of the ORC unit with a reduced HTF mass flow rate leads to a dual effect on the system performance: a decrease in the net energy conversion efficiency, and a reduction in the HTF outlet temperature, and thus in the mean cold tank temperature.

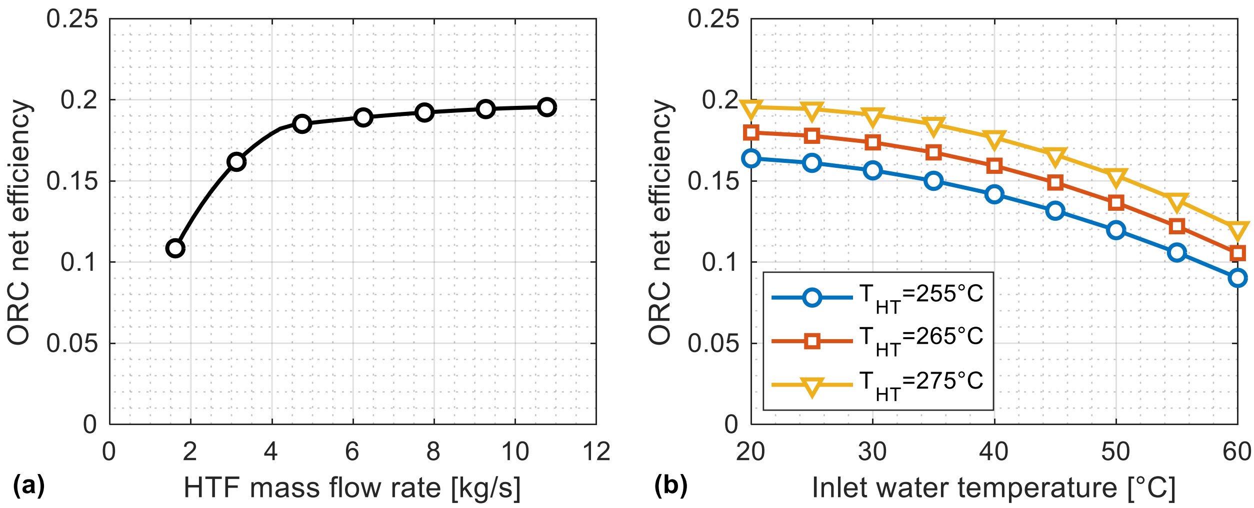

Figure 3 – Effects of (a) HTF mass flow rate and (b) HTF inlet temperature and inlet water temperature on the net efficiency of the ORC.

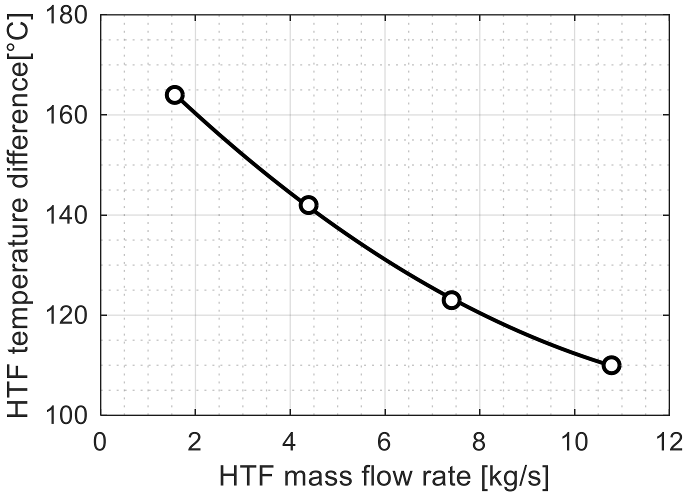

Figure 4 – Effect of HTF mass flow rate on the HTF temperature difference between the ORC inlet and outlet side.

3. Results and discussion

In this section the results obtained for different sizes of the biogas production section are reported and discussed. As mentioned above, the main parameters used for the design of this section are the biogas boiler thermal power $\dot{Q}^{d}_{BB}$, and the corresponding daily operating time Δt_{BB}. The effects of these parameters on the volume of the AD and the biogas storage are shown in Figure 5. Obviously, an increase in both the size of the biogas boiler (shown in Figure 5 as percentage of the thermal power input of the ORC) and its operating time leads to an increase in the required biogas flow rate, and consequently in the volume of the digester . It is worth noting that the mass flow rate of the feeding substrate depends on the volume of the reactor, meaning that large amounts of FVW need to be available to supply the AD for very large reactor volumes.

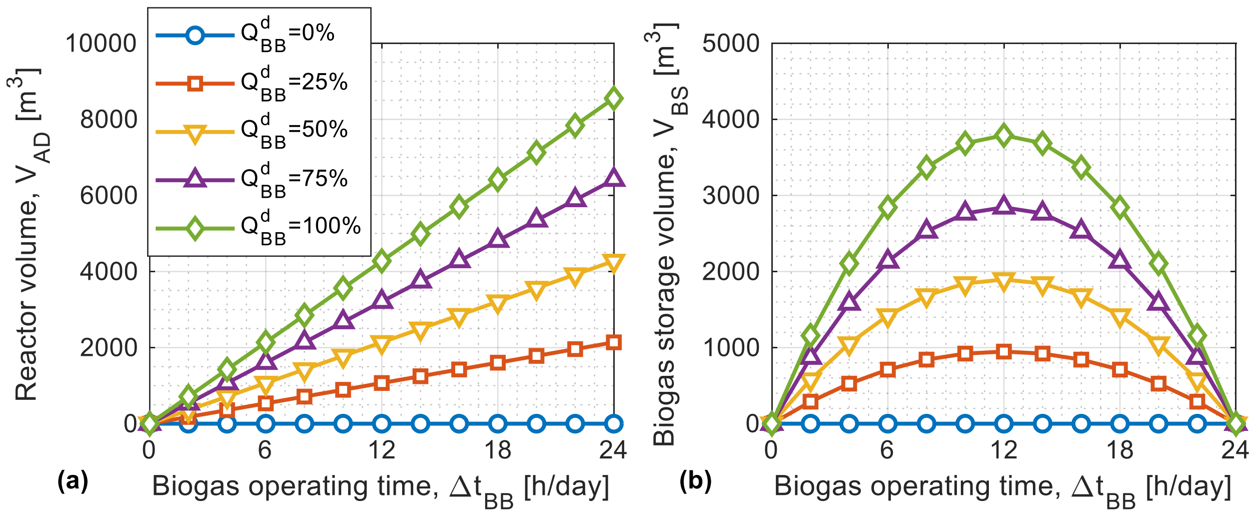

Figure 5 – Volumes of (a) the anaerobic digester (V_{AD}) and (b) biogas storage required (V_{BS}) as a function of biogas operating time (Δt_{BB}) and biogas boiler size ($\dot{Q}^{d}_{BB}$).

As shown in Figure 5(b), apart from the case of continuous biogas boiler operation (Δt_{BB}=24h), intermittent operation of the biogas boiler requires careful design of the biogas storage section. For a given value of $\dot{Q}^{d}_{BB}$, a decrease in the biogas boiler operating time leads to a decrease in the daily biogas consumption, but simultaneously leads to an increase in the biogas storage capacity since the AD operates 24 h per day. Overall, as shown in Figure 5(b), the biomass storage volume has a maximum value for Δt_{BB}=12h.

3.1. Annual performance

The main annual performance is evaluated using the meteorological dataset obtained using Meteonorm software for the location of Ottana. Based on the current plant performance (which includes only the CSP section), the expected production of solar field thermal energy during a typical year is about 5.2 GWh, with a plant capacity factor of about 16% and a yearly ORC operating time of lower than 1700 h. A significant improvement in the plant operating time can be achieved by the hybridisation of the plant through the introduction of the biogas section. The results of applying two different operating strategies in the hybrid system are presented and discussed in the following sections.

3.1.1. Biogas priority case

Figure 6 illustrates the hybrid plant capacity factor and the yearly ORC operating time as a function of the biogas boiler size and operating time. As can be seen from Figure 6 (a), the highest capacity factors (about 93%) are obtained for continuous operation of the biogas boiler (Δt_{BB}=24h). However, even with a continuous biogas boiler operation, a 100% capacity factor cannot be reached due to the degradation in ORC performance at high ambient temperatures, and especially in summer. Furthermore, as shown in Figure 6(b), a significant rise in the ORC operating time can be achieved from hybridisation of the CSP plant. In particular, a marked increase in the operating time is observed for a biogas boiler of size greater than 40% $\dot{Q}^{d}_{ORC}$ (very noticeable for Δt_{BB}=24h). In this case, the HTF mass flow rate produced by the biogas boiler is equal to the minimum HTF mass flow rate required by the ORC, with the possibility of directly feeding the turbo generator if the temperature in the cold tank equals the design temperature (165°C). However, this does not result in a corresponding increase in the capacity factor. In fact, in the case of a biogas boiler sized for the ORC minimum load, two main effects influence the system performance and thus the plant capacity factor: (i) a reduction in the cold tank temperature due to the higher HTF temperature difference occurring at the ORC evaporator (as shown in Figure 4); and (ii) a reduction in the ORC net efficiency. In particular, Figure 7(a) shows the influence of the power and operating time of the biogas boiler on the ORC conversion efficiency. In general, an increase in the mean ORC efficiency is observed with a rise in both the size of the biogas boiler and its operating time, thanks to the higher thermal power availability (both in terms of HTF mass flow rate and hot tank temperature) and the consequent reduction in the use of the ORC unit under part-load conditions. However, as already observed in the previous figure, a discontinuity occurs at a value of $\dot{Q}^{d}_{BB}$ equal to about 40% of $\dot{Q}^{d}_{ORC}$, with an important reduction in the ORC efficiency. In fact, in this case, the biogas boiler is able to directly supply the ORC unit, but the latter very often operates at its minimum load.

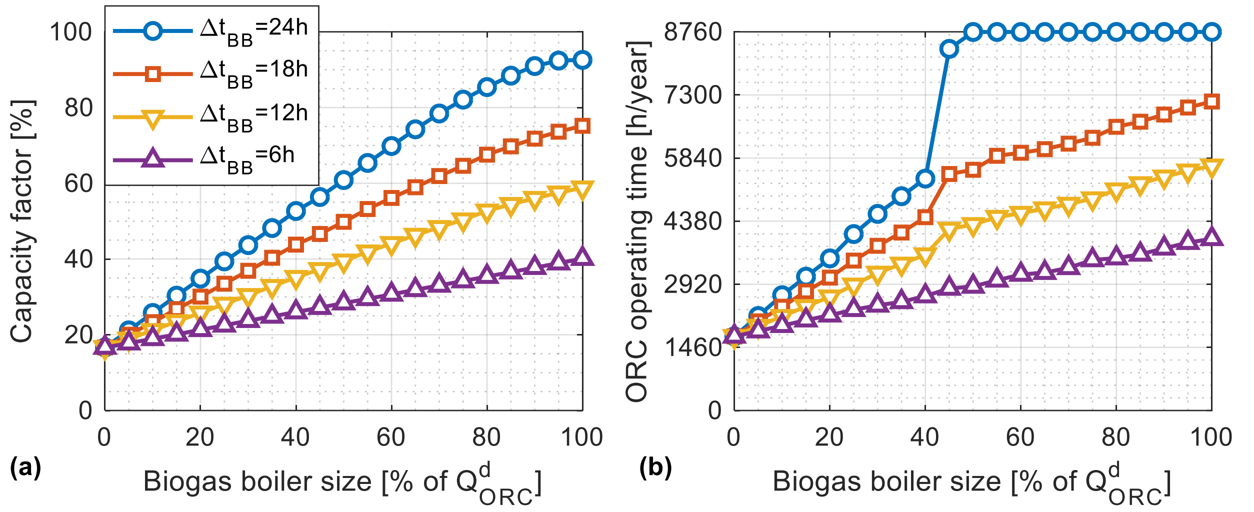

Figure 6 – (a) Plant capacity factor and (b) yearly ORC operating time as a function of the size and operating time (Δt_{BB}) of the biogas boiler.

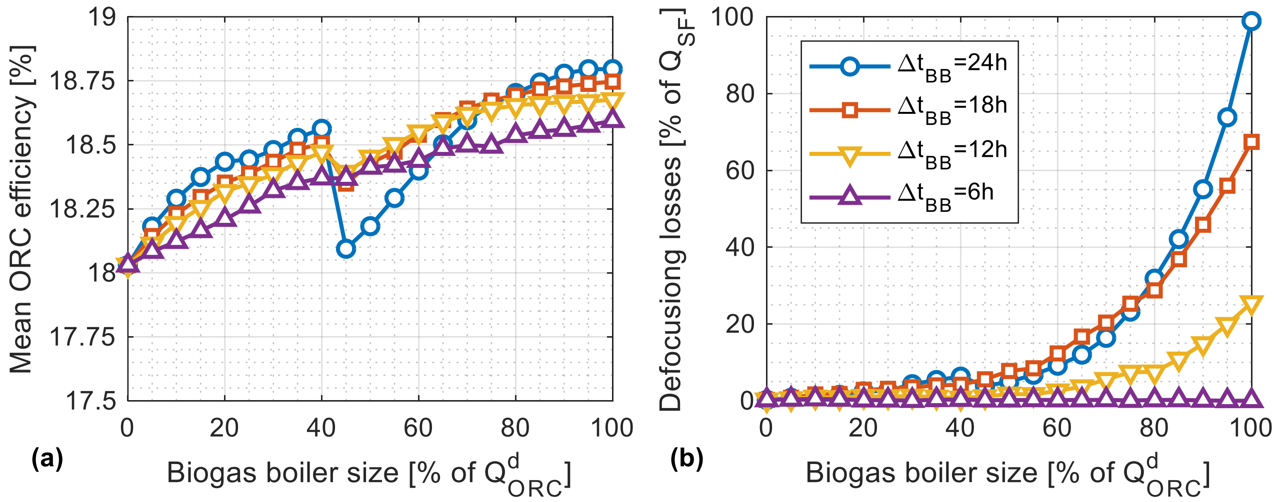

Figure 7 – (a) Annual average ORC efficiency and (b) solar field defocusing losses as a function of the size and operating time(Δt_{BB}) of the biogas boiler.

Another important aspect that strongly affects the performance of the hybrid plant involves the storage capacity of the TES system, which was originally designed for the CSP section alone. However, the additional thermal energy produced by the biogas section and sent to the TES system increases the number of times the hot tank overcharges, and hence the requirements for energy curtailment of the solar field energy production, in the case where a biogas priority strategy is chosen. In this regard, Figure 7(b) shows the annual energy losses due to mirror defocusing, expressed as a percentage of the expected annual solar field energy production. As can be observed from the figure, the main defocusing losses occur at high values of the biogas boiler power and for continuous biogas boiler operation, reaching 100% defocusing losses at $\dot{Q}^d_{BB}=\dot{Q}^d_{ORC}$. In the latter case, no energy is produced by the solar field, since the ORC unit is only supplied by the biogas system. This is an unwanted drawback of the strategy adopted for the management of the TES section, which gives priority to biogas production rather than the solar field. Minor solar field energy curtailments are observed for values of Δt_{BB} lower than 12–18 h, even for high values of the biogas boiler power output.

3.1.2. *Solar priority case*

As observed in the previous section, a possible drawback of hybridising CSP plants is the risk of frequent overcharging of the TES system during high insulation periods. The biogas priority strategy manages this overproduction by reducing the solar field thermal power through mirror defocusing. Conversely, the solar priority strategy reduces the thermal power delivered by the biogas boiler, with a consequent reduction in its HTF mass flow rate production. This approach allows to also exploit the storage capacity of the biogas storage (if present), since any biogas not burned can be stored and used in a subsequent period. Obviously, since the biogas digester operates at a constant mass flow rate, overcharging of the biogas storage could arise from adopting a solar priority strategy, and flaring of a portion of the biogas produced via anaerobic digestion may therefore be required to avoid overpressures in the biogas vessel.

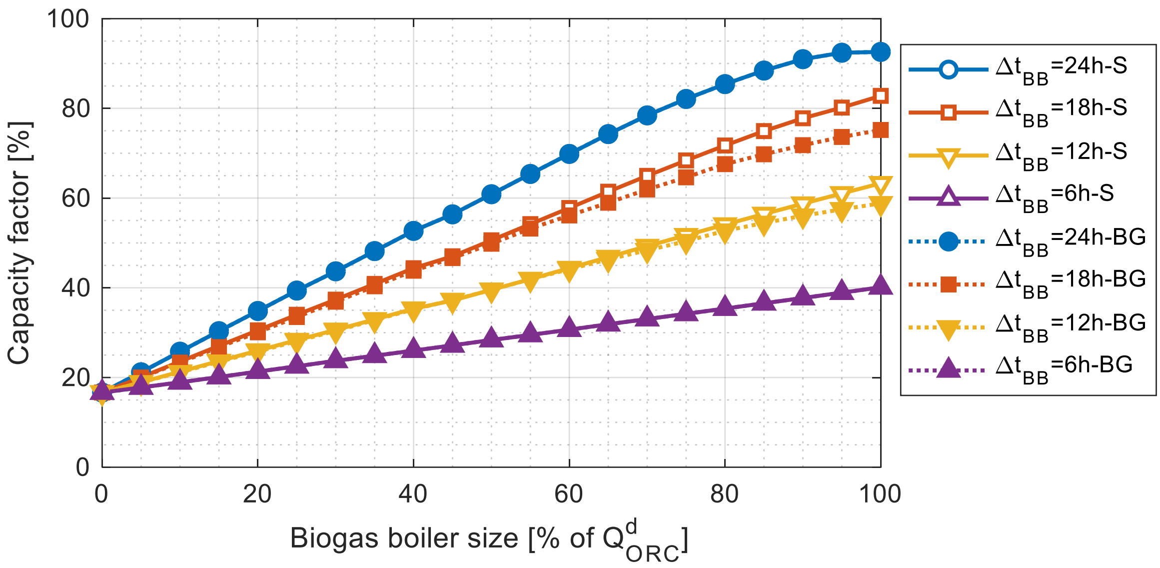

Figure 8 – Comparison of the plant capacity factor obtained by following a biogas priority strategy (BG) and a solar priority strategy (S) as a function of the size and operating time (Δt_{BB}) of the biogas boiler.

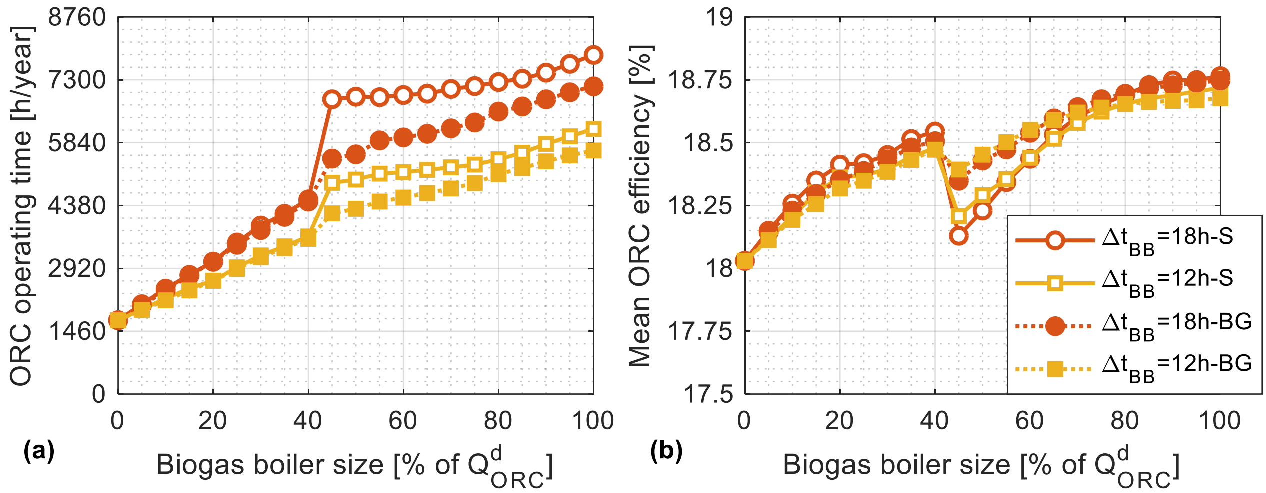

Figure 9 – Comparison of the (a) ORC operating time and (b) ORC efficiency obtained by following a biogas priority strategy and a solar priority strategy as a function of the biogas boiler size and biogas operating time (Δt_{BB}).

The results for the plant capacity factor obtained by following the solar priority strategy are shown in Figure 8, and are compared with those achieved by the biogas priority strategy. As expected, no difference is found in the case of 24-hour operation of the biogas boiler, since, as shown in Figure 5(b), no biogas storage is introduced for these design conditions, regardless of the size of the biogas boiler. There is also no variation in the system performance for the case $\Delta t_{BB} = 6$ h, where the low use of biogas results in a very low risk of TES overcharging and therefore negligible defocusing losses. Conversely, an increase in the plant capacity factor is obtained by using the solar priority strategy for the cases $\Delta t_{BB} = 12$ h and $\Delta t_{BB} = 18$ h, compared with the performance obtained in the previous section. The increase in the plant capacity factor becomes more and more noticeable with the increasing size of the biogas boiler, reaching seven percentage points for a size of 100% of the nominal ORC thermal power input. This improvement in the system performance is mainly due to better management of the two storage systems, which leads to a rise in the thermal energy available for the ORC unit and a consequent increase in the ORC annual operating time. This is illustrated in Figure 9(a), where, starting with a biogas boiler of size equal to 40% of $\dot{Q}^{d}_{ORC}$, a positive deviation from the ORC operating time obtained with the biogas priority strategy is observed. Conversely, a degradation of the mean ORC efficiency is shown in Figure 9(b), in particular for a biogas boiler with size in the range of 40%–60% of the design value for the ORC thermal power input. Under these conditions, the change in the plant management allows to increase the operating time of the ORC unit at its minimum part load, with a consequently lower conversion efficiency. In addition to the variations in the plant capacity factor, the introduction of a different operating strategy leads to variations in the losses produced by overcharging of the storage system. Unlike in the previous section, there is a curtailment in the energy produced from biogas (due to biogas flaring) by following the solar priority strategy, when both the hot tank and the biogas storage system are fully charged, and the biogas produced by the anaerobic digestion is neither used nor stored. However, as shown in Figure 10(a), mirror defocusing is still required in the solar priority case in order to maintain the mass balance of the hot tank during periods of very high availability of solar energy, even if the solar field energy production must be reduced only after the shutting down of the biogas boiler. Unlike in the biogas priority scheme, these losses are strongly reduced, reaching a maximum of 5% of the yearly energy produced by the solar field. On the other hand, as shown in Figure 10(b), there is a significant reduction in the potential energy produced by the biogas section for the case $\Delta t_{BB} = 24$ h, that is, when the biogas storage is not included and almost 20% of the biogas must be sent for flaring for a biogas boiler of large size. A biogas energy curtailment is also observed for the case $\Delta t_{BB} = 18$ h, although these losses are observed only for large biogas boiler sizes, reaching a maximum value of 5% of the overall biogas energy production.

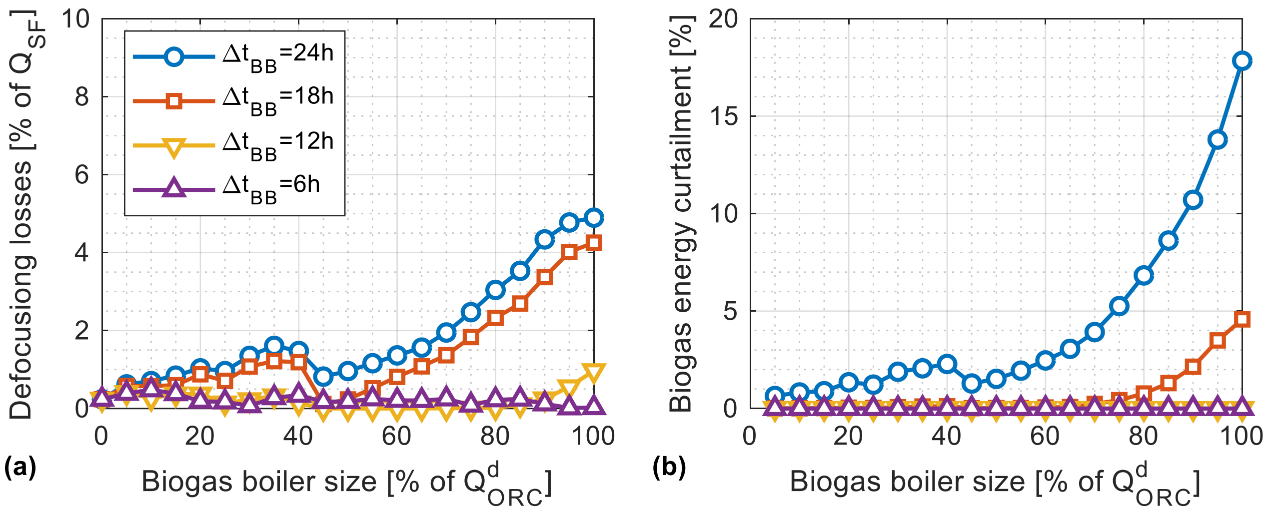

Figure 10 – (a) Solar field defocusing losses and (b) biogas energy curtailment as a function of the size and operating time (Δt_{BB}) of the biogas boiler.

3.2. Preliminary economic analysis

Finally, the cost-effectiveness of the hybridisation of existing CSP plants with biogas systems is evaluated using a marginal economic metric. The marginal levelised cost of energy ($LCOE_M$) is used as the main economic index, and is calculated as:

$$LCOE_M = \frac{IC_{BG} + \sum_{n=1}^{N} \frac{AC_{BG}}{(1+i)^n}}{\sum_{n=1}^{N} \frac{E_{CSP+BG} - E_{CSP}}{(1+i)^n}} \tag{16}$$

where IC_{BG} are the initial costs related to the additional capital investments required by the biogas section, AC_{BG} are the annual costs associated with the operation of the biogas section (including the biomass costs), E_{CSP+BG} is the expected annual electrical energy produced by the hybrid CSP-biogas plant, E_{CSP} is the annual electrical energy produced by the CSP section alone, i is the interest rate and N is the plant lifetime in years. The initial and annual costs are calculated as:

$$IC_{BG} = c_{AD}V_{AD} + c_{BS}V_{BS} + c_{BB}\dot{Q}_{BB}^{d} \tag{17}$$

$$AC_{BG} = c_{O\&M} IC_{BG} + c_{FVW} \sum_{t=1}^{8760} \dot{m}_{FVW} \quad (18)$$

where c_{AD}, c_{BS} and c_{BB} are the specific costs of the anaerobic digester, biogas storage and biogas boiler respectively, $c_{O\&M}$ are the annual operating and maintenance costs (expressed as a percentage of the initial costs), and c_{FVW} is the specific FVW cost (including transportation). This economic analysis was applied to the existing Ottana solar facility, and Table 3 lists the main assumptions used for the calculation of the marginal LCOE. Figure 11 shows the marginal LCOE for different values of the size and operating time of the biogas boiler, following the two proposed operating strategies (biogas priority and solar priority). Continuous use of the biogas boiler (Δt_{BB}=24h) gives the lowest marginal LCOE, except at high values of the biogas boiler power, where the influence of the energy curtailment becomes predominant and a decrease in the biogas operating time is recommended from an economic point of view. For a biogas boiler with a size in the range 80%–100% of the design ORC thermal input, the lowest marginal LCOE is reached by using the biogas boiler 18 h per day and following a solar priority strategy. A further decrease in the daily utilisation time of the biogas boiler is not convenient, although it can avoid the need for energy curtailment.

Overall, the lowest marginal cost is reached for a biogas boiler of size equal to about 500 kW (15% of $\dot{Q}_{ORC}^{d}$). However, only minor changes in the marginal LCOE are observed for sizes of up to 65% of $\dot{Q}_{ORC}^{d}$. In fact, the marginal LCOE values obtained in these cases vary from 141.6 €/MWh to 146.6 €/MWh, and a more detailed economic analysis is required to determine the most profitable biogas configuration. On the other hand, Figure 11 demonstrates that the greatest economic benefits from the hybridisation of a CSP plant with a biogas plant are obtained from the introduction of a biogas section that is able to guarantee continuous operation of the power block under minimum part-load conditions. The marginal LCOE values obtained in these cases are in line with typical LCOE values achieved by biogas systems based on anaerobic digestion (120–150 €/MWh [25]). It is worth noting that the investment cost for the CSP plant at the Ottana solar facility was around 5 M€ (without considering civil construction works), with an expected annual electrical energy production of about 0.92 GWh. Hence, the current LCOE without considering annual costs is about 515 €/MWh. The marginal LCOE obtained, which represents the cost of the additional energy produced via hybridisation, is about one third of the current energy production cost.

Finally, it is important to highlight the amount of fruit and vegetable waste required by the anaerobic digester in order to guarantee the desired production of biogas. Figure 12 shows the daily demand for FVW as a function of the biogas boiler size and the operating time, which is independent of the operating strategy chosen. If the optimal design is chosen for the biogas section from an economic point of view, a daily amount of FVW of about 40 t/day is required. Obviously, a lack of FVW availability could be a strong constraint on the hybridisation of the CSP plant, and a detailed investigation of the availability of waste resources around the location of the plant is therefore required.

Table 3 – Main cost assumptions [24–26].

Initial costs		**Annual costs**	
Anaerobic digester (c_{AD})	450 €/m^3	O&M ($c_{O\&M}$)	3% of IC_B
Biogas storage (c_{BS})	40 €/m^3	FVW cost (c_{FVW})	4 €/t
Biogas boiler (c_{BB})	180 €/kW	**Other parameters**	
		Annual interest rate (i)	7%
		Plant operational lifetime (N)	20 years

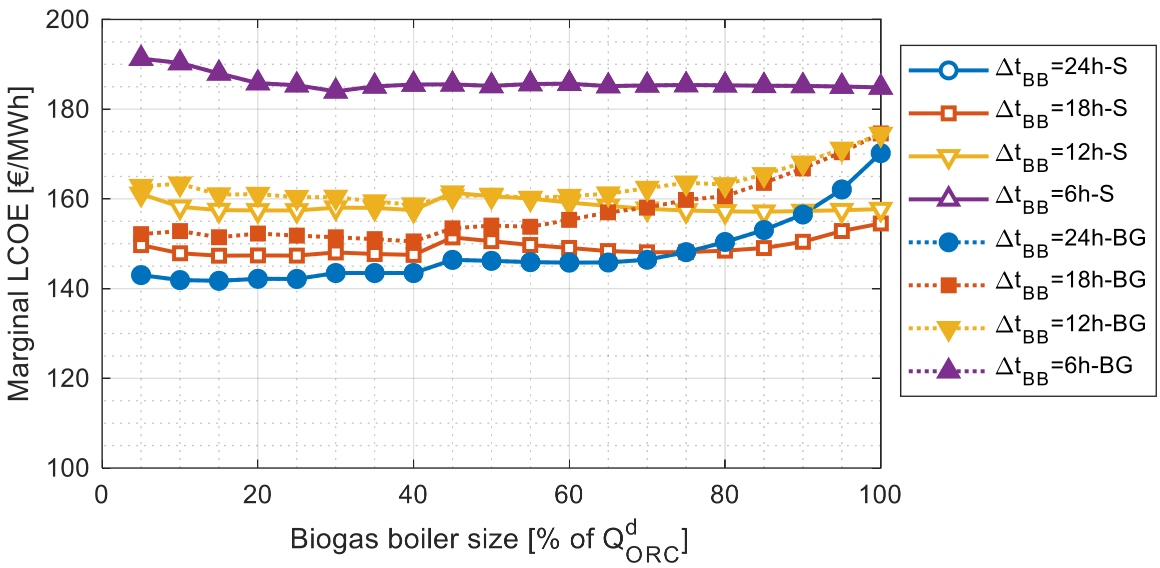

Figure 11 – Marginal levelised cost of energy obtained by following a biogas priority strategy (BG) and a solar priority strategy (S) as a function of the biogas boiler size and biogas operating time (Δt_{BB}).

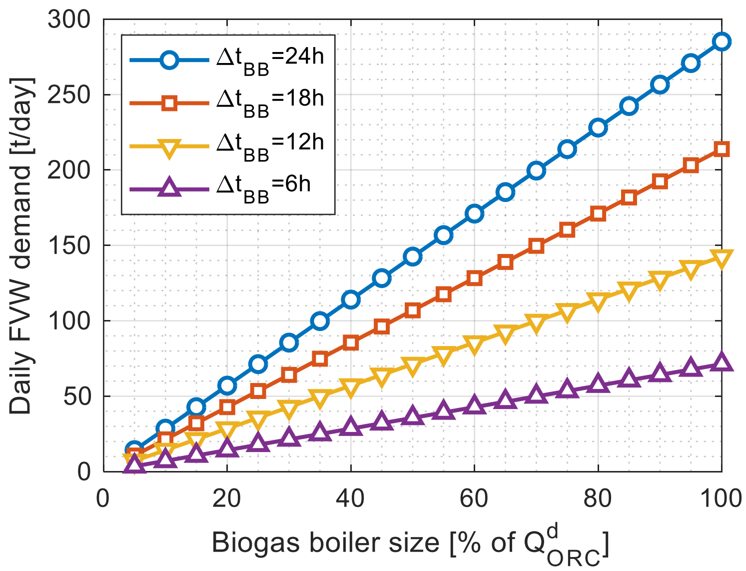

Figure 12 - Daily FVW demand as a function of the biogas boiler size and biogas operating time (Δt_{BB}).

4. Conclusions

The capabilities of hybrid CSP-biogas plants were assessed in this study based on technical and economic performance metrics, and a case study of the existing solar ORC system of the Ottana solar facility was presented. The latter includes linear Fresnel collectors integrated with a double-tank thermal energy storage system, and uses thermal oil as heat transfer fluid and storage medium. Here, a parallel hybridisation concept with a biogas section was considered, in which the biogas is produced by an anaerobic digester coupled with a suitable biogas storage system.

To properly size the biogas section, two main design parameters were introduced: the power of the biogas boiler and its daily operating time. The main annual performance of the hybrid CSP-biogas plant was investigated by varying these two parameters. Starting with the expected performance for the current plant configuration of the Ottana solar facility (with only the CSP section), significant improvements in the plant capacity factor and in the overall ORC efficiency can be achieved by hybridisation with biogas. However, oversizing of the biogas section results in a remarkable increase in the energy curtailment of the solar field and/or biogas energy production, due to the restricted TES capacity and consequent degradation in the plant's performance. This drawback could be counteracted by the implementation of a suitable operating strategy. In particular, the results of this study demonstrate that the use of a solar priority strategy in which the biogas power production is mainly managed in order to avoid overcharging the TES systems can achieve better performance in terms of minimising the energy curtailment, allowing to better exploit the biogas storage capacity, if present.

The best configuration, even from an economic point of view is achieved by a biogas boiler that is designed for continuous operation and is a suitable size to supply part (in the range 10%–65%) of the nominal thermal power input required by the ORC unit. The marginal LCOE values obtained in these cases (141.5–146.5 €/MWh) are in line with typical LCOE values for biogas systems based on anaerobic digestion (120–150 €/MWh).

However, in-depth economic analyses will be required in the future to determine the optimal biogas boiler size based on variations in the sale price of electricity, which could reward flexible operation strategies and the operability of the biogas boiler under part-load conditions. In fact, these hybrid CSP-biogas power plants can improve their profitability thanks to their ability of providing ancillary services to the grid as well as to operate in electric load following mode.

Acknowledgements

This paper forms part of a research project funded by P.O.R. SARDEGNA F.S.E. 2014-2020 - Axis III Education and Training, Thematic Goal 10, Specific goal 10.5, Action partnership agreement 10.5.12 – "Call for funding of research projects – Year 2017".

References

[1] European Commission. Initiative for Global Leadership in Concentrated Solar Power -- Implementation Plan 2017:66.

[2] Stekli J, Irwin L, Pitchumani R. Technical Challenges and Opportunities for Concentrating Solar Power With Thermal Energy Storage. J Therm Sci Eng Appl 2013;5:021011. doi:10.1115/1.4024143.

[3] Powell KM, Rashid K, Ellingwood K, Tuttle J, Iverson BD. Hybrid concentrated solar thermal power systems: A review. Renew Sustain Energy Rev 2017;80:215–37. doi:10.1016/j.rser.2017.05.067.

[4] Behar O, Kellaf A, Mohamedi K, Belhamel M. Instantaneous performance of the first integrated solar combined cycle system in Algeria. Energy Procedia 2011;6:185–93. doi:10.1016/j.egypro.2011.05.022.

[5] Pramanik S, Ravikrishna R V. A review of concentrated solar power hybrid technologies. Appl Therm Eng 2017;127:602–37. doi:10.1016/j.applthermaleng.2017.08.038.

[6] Hussain CMI, Norton B, Duffy A. Technological assessment of different solar-biomass systems for hybrid power generation in Europe. Renew Sustain Energy Rev 2017;68:1115–29. doi:10.1016/J.RSER.2016.08.016.

[7] Peterseim JH, Herr A, Miller S, White S, O'Connell DA. Concentrating solar power/alternative fuel hybrid plants: Annual electricity potential and ideal areas in Australia. Energy 2014. doi:10.1016/j.energy.2014.02.068.

[8] San Miguel G, Corona B. Hybridizing concentrated solar power (CSP) with biogas and biomethane as an alternative to natural gas: Analysis of environmental performance using LCA. Renew Energy 2014;66:580–7. doi:10.1016/j.renene.2013.12.023.

[9] Bai Z, Liu Q, Lei J, Wang X, Sun J, Jin H. Thermodynamic evaluation of a novel solar-biomass hybrid power generation system. Energy Convers Manag 2017. doi:10.1016/j.enconman.2017.03.028.

[10] Suresh NS, Thirumalai NC, Dasappa S. Modeling and analysis of solar thermal and biomass hybrid power plants. Appl Therm Eng 2019. doi:10.1016/j.applthermaleng.2019.114121.

[11] Pantaleo AM, Camporeale SM, Sorrentino A, Miliozzi A, Shah N, Markides CN. Hybrid solar-biomass combined Brayton/organic Rankine-cycle plants integrated with thermal storage: Techno-economic feasibility in selected Mediterranean areas. Renew Energy 2020;147:2913–31. doi:10.1016/j.renene.2018.08.022.

[12] Sterrer R, Schidler S, Schwandt O, Franz P, Hammerschmid A. Theoretical Analysis of the Combination of CSP with a Biomass CHP-plant Using ORC-technology in Central Europe. Energy Procedia 2014;49:1218–27. doi:10.1016/j.egypro.2014.03.131.

[13] Pantaleo AM, Camporeale SM, Miliozzi A, Russo V, Shah N, Markides CN. Novel hybrid CSP-biomass CHP for flexible generation: Thermo-economic analysis and profitability assessment. Appl Energy 2017;204:994–1006. doi:10.1016/j.apenergy.2017.05.019.

[14] Milani R, Szklo A, Hoffmann BS. Hybridization of concentrated solar power with biomass gasification in Brazil's semiarid region. Energy Convers Manag 2017. doi:10.1016/j.enconman.2017.04.015.

[15] Oyekale J, Heberle F, Petrollese M, Brüggemann D, Cau G. Biomass retrofit for existing solar organic

Rankine cycle power plants: Conceptual hybridization strategy and techno-economic assessment. Energy Convers Manag 2019;196:831–45. doi:10.1016/j.enconman.2019.06.064.

[16] Corré WJ, Conijn JG. Biogas from Agricultural Residues as Energy Source in Hybrid Concentrated Solar Power. Procedia Comput Sci 2016;83:1126–33. doi:10.1016/j.procs.2016.04.233.

[17] Mishra A, Chakravarty MN, Kaushika ND. Thermal optimization of solar biomass hybrid cogeneration plants. J Sci Ind Res 2006;65:355–63.

[18] Zhang G, Li Y, Dai YJ, Wang RZ. Design and analysis of a biogas production system utilizing residual energy for a hybrid CSP and biogas power plant. Appl Therm Eng 2016;109:423–31. doi:10.1016/J.APPLTHERMALENG.2016.08.092.

[19] Colmenar-Santos A, Bonilla-Gómez J-L, Borge-Diez D, Castro-Gil M. Hybridization of concentrated solar power plants with biogas production systems as an alternative to premiums: The case of Spain. Renew Sustain Energy Rev 2015;47:186–97. doi:10.1016/J.RSER.2015.03.061.

[20] Soares J, Oliveira AC. Numerical simulation of a hybrid concentrated solar power/biomass mini power plant. Appl Therm Eng 2017. doi:10.1016/j.applthermaleng.2016.06.180.

[21] Petrollese M, Cau G, Cocco D. The Ottana solar facility: dispatchable power from small-scale CSP plants based on ORC systems. Renew Energy 2020;147:2932–43. doi:10.1016/j.renene.2018.07.013.

[22] Cau G, Cocco D. Comparison of medium-size concentrating solar power plants based on parabolic trough and linear Fresnel collectors. Energy Procedia 2014;45:101–10. doi:10.1016/j.egypro.2014.01.012.

[23] Forristall R. Heat Transfer Analysis and Modeling of a Parabolic Trough Solar Receiver Implemented in Engineering Equation Solver. 1617 Cole Boulevard Golden, Colorado 80401-3393 NREL: 2003. doi:NREL/TP-550-34169.

[24] Scano EA, Asquer C, Pistis A, Ortu L, Demontis V, Cocco D. Biogas from anaerobic digestion of fruit and vegetable wastes: Experimental results on pilot-scale and preliminary performance evaluation of a full-scale power plant. Energy Convers Manag 2014;77:22–30. doi:10.1016/J.ENCONMAN.2013.09.004.

[25] International Renewable Energy Agency (IRENA). Biomass from Power Generation. 2012.

[26] Akbulut A. Techno-economic analysis of electricity and heat generation from farm-scale biogas plant: Çiçekdağı case study. Energy 2012;44:381–90. doi:10.1016/J.ENERGY.2012.06.017.